Vector Control of Interior Permanent Magnet Synchronous Motor over Wide range of Speed using Fuzzy Logic Controller

Jaydeepsinh C. Baria[1], Kuldip Patel[2], Darshankumar C. Dalwadi[3]

[1] *Research scholar, Gujarat Technological University, India, jcbaria1982@gmail.com*

[2] *with the BVM Engineering College, India patelkuldip10a42@gmail.com).*

[3] *Associate Professor BVM Engineering College, India darshan.dalwadi@bvmengineering.ac.in).*

Abstract

This paper proposed the fuzzy logic controller (FLC) which can control the speed and torque of Interior Permanent Magnet Synchronous Motor (IPMSM) Drives. The Input to the FLC is Speed Error, Change in Speed Error, and Actual Speed. The Output of the FLC is d-axis current (I_d) and q-axis current (I_q). The proposed FLC can control the Torque and Flux simultaneously such that we can get desired speed. This FLC is designed based on the Maximum Torque per Ampere (MTPA) method stand-still to base speed operation and Field Weakening (FW) Method for the above base speed operation. The hysteresis current control method is used for generating the pulses for the Inverter. This whole drive system is simulated in MATLAB-Simulink Software. The robustness of the controller can be realized by the results. The propose system is applicable to Electric Vehicle (EV), Air Conditioners (AC) etc.

Keywords*:* *Interior Permanent Magnet Synchronous Motor (IPMSM), Fuzzy Logic Controller (FLC), Maximum Torque per Ampere (MTPA), Field Weakening (FW), Vector Control, Hysteresis Current Controller.*

1. Introduction

IPMSM has been introduced in the year of 2001 and it is widely accepted now as an efficient alternative to AC Induction Motor. In these years, a lot of research has been done on IPMSM's efficiency, performance, and applications. The most obvious reason for this is that IPMSM offers high efficiency, control over a wide range of speeds, and high-power density. Interior Permanent Magnet Synchronous Motor (IPMSM) is the best choice for loads like Electric Vehicles, Elevators, and Traction in which space limitations are important. [1]-[8]

IPMSM offers better control over a wide speed range. This is done by Maximum Torque Per Ampere (MTPA) and Field Weakening (FW) algorithms. We control the speed from zero to base speed by MTPA and beyond the base speed by FW methodology.[4]-[8] IPMSM have a permanent-magnets buried inside the rotor structure. Its rotor surface becomes smooth and the air gap will be reduced. Therefore, it is suitable for high-speed operation. The d-axis inductance and q-axis inductance is not equal for IPMSM. It will give us an extra torque produced by d-axis current called Reluctance Torque.[9] Therefore,

In MTPA, we get maximum torque per unit current, this is how we can reduce the copper loss in IPMSM is minimum and we get better efficiency.[4],[6] We will reduce the flux by negative d-axis current to go beyond the base speed operation. The motor parameters play crucial role in FW region because the voltage constrain in depends on the motor parameter.[5]
The rotor core around the permanent magnets is saturated. The armature reaction affects the air gap flux in IPMSM. Due to this the reluctance parameters of IPMSM are varied. Hence the dynamic and steady state performance of IPMSM is affected. Its control in high performance industrial applications requires especial attention.[5][6]

The conventional controller used to control the IPMSM is PI or PID controller. It requires the exact mathematical model of IPMSM. However, it is difficult to derive exact mathematical model of IPMSM due to saturation, armature reaction, dynamic loading, and temperature variation. In this paper we propose fuzzy logic controller to overcome above limitations. As Fuzzy Set theory introduced by L. Zadeh, a Fuzzy logic Controller have following advantages: (1) It does not require an exact Mathematical Model. (2) It is based on the linguistic rules with an IF-THEN general structure, which is basis of human logic. (3) It can handle any non-linearity of system.
The complete vector control scheme of IPMSM drive including fuzzy logic controller is simulated in MATLAB SIMULINK.

Nomenclature
R_S - Per phase Stator Resistance
i_d – d-axis stator current
i_q - q-axis stator current
L_d – d-axis stator inductance
L_q – q-axis stator inductance
ω_e – rotor speed
Φ_d – flux linkage along d-axis
Φ_q - flux linkage along q-axis
Φ_{PM}- flux linkage due to Permanent Magnet
P – Number of Pole Pairs
θ_r- phase shift

2. Mathematical Model of IPMSM

The mathematical model for the vector control of the IPMSM can be derived from its dynamic d-q model which can be obtained from well-known model of the induction machine with the equation of damper winding and field current dynamics removed. The synchronously rotating rotor reference frame is chosen so the stator winding quantities are transformed to the synchronously rotating reference frame that is revolving at rotor speed. The consequences is that there is zero speed differential between the rotor and stator magnetic fields. the stator q and d axis windings have a fixed phase relationship with the rotor magnet axis which is the d axis in the modelling. A mathematical model of the

IPMSM is used in order to simulate the behavior of the machine in Matlab/Simulink. The model is expressed in the dq rotor reference frame, where the d axis is aligned with the rotor flux-linkage as shown in Fig.1.[11][12]

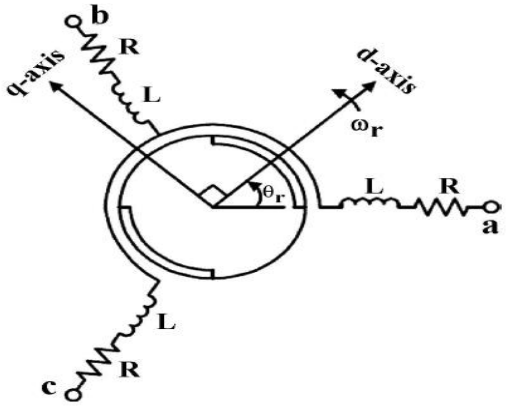

Figure 1. The Vector Diagram for DQ transformation [13]

The stator voltages for 3 phases can be written as below:

$$v_a = R_s i_a + L_s \frac{d}{dt} i_a - \omega_e \Phi_{PM} sin(\theta_r) \quad (1)$$

$$v_b = R_s i_b + L_s \frac{d}{dt} i_b - \omega_e \Phi_{PM} sin\left(\theta_r - \frac{2\pi}{3}\right) \quad (2)$$

$$v_c = R_s i_c + L_s \frac{d}{dt} i_c - \omega_e \Phi_{PM} sin\left(\theta_r + \frac{2\pi}{3}\right) \quad (3)$$

The equation (4) and (5) are Dynamic equations of IPMSM in synchronously rotating d-q referencing frame is obtain by clerk-perk transformation. Some assumptions will be taken for convenience.

- The induced EMF is Sinusoidal.
- Saturation and Core losses in rotor are negligible.
- There is no damper winding on rotor.

$$v_d = R_S i_d + L_d \frac{di_d}{dt} - \omega_e \Phi_q \quad (4)$$

$$v_q = R_S i_q + L_q \frac{di_q}{dt} + \omega_e \Phi_d \quad (5)$$

$$\Phi_d = L_d i_d + \Phi_{PM} \quad (6)$$

$$\Phi_q = L_q i_q \quad (7)$$

The Equivalent circuit of the PMSM in DQ- axis derived using DQ modeling method is shown in Fig-2.

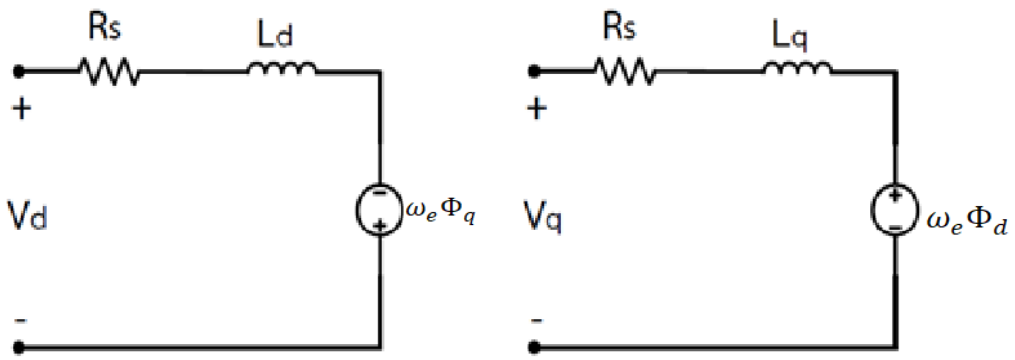

Figure 2. The PMSM equivalent circuit in the DQ-axis [13]

$$T_e = \frac{3P}{2}(\Phi_{PM} i_q + (L_d - L_q) i_d i_q) \quad (8)$$

The first term in Equation (8) represents the torque due to permanent magnet buried in rotor, and the second term represents the reluctance torque developed due to interaction of d- axis and q-axis current.

3. MTPA and FW Topology

3.1 Maximum torque per Ampere (MTPA) Control: [2]

Maximum torque per Ampere control generates the reference d axis current (i_d) and q axis current (i_q), to produce maximum torque per unit current. The condition for MTPA trajectory can be derived from the Equation (8) as follows.

$$\frac{\partial T_e}{\partial i_q} = 0$$

$$\Phi_{PM} + (L_d - L_q) i_q \frac{\partial T_e}{\partial i_q} + (L_d - L_q) i_d = 0 \quad (9)$$

The relation between stator phase current and current in d-q reference frame is

$$i_s = \sqrt{i_d^2 + i_q^2} \quad (10)$$

Using equation (8)

$$\frac{\partial i_d}{\partial i_q} = -\frac{i_q}{i_d} \quad (11)$$

Solving equations (7) and (9)

$$i_d = \frac{\Phi_{PM}}{2(L_d - L_q)} + \sqrt{\frac{{\Phi_{PM}}^2}{4(L_d - L_q)^2} + i_q^2} \quad (12)$$

The trajectory of MTPA curve, the voltage limit ellipse, the current limit curve and constant torque curves are shown in Figure (3).

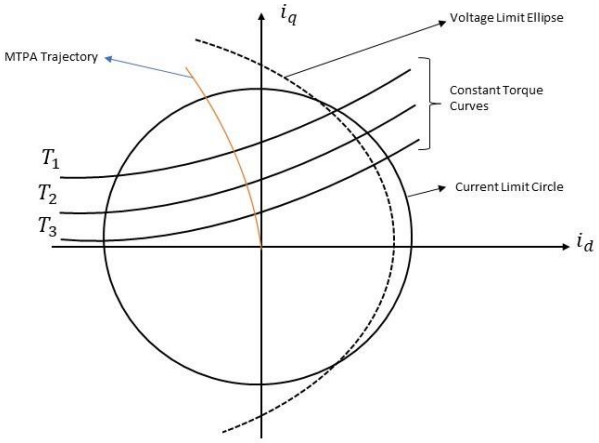

Figure 3 Limit Curves in MTPA operating Region

The voltage constrain for the drive system is satisfied for below base speed operation. The operating point of the drive system is located along the MTPA trajectory shown in Figure (3). The intersecting point of constant torque curve and MTPA trajectory is the operating point, which is at minimum distance from the origin. This distance represents the stator current. In other words, MTPA trajectory leads to the required torque by minimum current. Therefore, the copper loss is reduced and the efficiency of drive system can be maximized.

3.2 Field Weakening (FW) Control:[3]

When we operate our motor beyond the rated speed, we need to care about the Voltage and Current constraints [3]. The Current constraint and Voltage constraint is expressed using Equation (10) and (11) respectively.

$$I_s = \sqrt{I_d^2 + I_q^2} \leq I_{sm} \quad (13)$$

$$V_s = \sqrt{v_d^2 + v_q^2} \leq V_{sm} \quad (14)$$

Where, I_{sm} and V_{sm} are available maximum current and voltage respectively.
Put values of v_d and v_d in equation (14), we get

$$V_s = \sqrt{(R_S i_d + L_d \frac{di_d}{dt} - \omega_e \Phi_q)^2 + (R_S i_d + L_d \frac{di_d}{dt} + \omega_e \Phi_d)^2} \leq V_{sm} \quad (15)$$

To make analysis simple, we consider only steady state terms in voltage constrain equation and ignoring the resistive drop.

$$V_s = \sqrt{(\omega_e \Phi_d)^2 + (\omega_e \Phi_d)^2} \leq V_{sm} \quad (16)$$

From Equation (7) and (8), we get

$$V_s = \sqrt{(\omega_e L_q i_q)^2 + (\omega_e (L_d i_d + \Phi_{PM}))^2} \leq V_{sm} \quad (17)$$

After simplification,

$$(L_q i_q)^2 + (L_d i_d + \Phi_{PM})^2 \leq \left(\frac{V_{sm}}{\omega_e}\right)^2 \quad (18)$$

Equation (13) represents the current limit circle with radius I_s and center at origin.

Equation (18) represents the voltage ellipse centered at $(0, -\frac{\Phi_{PM}}{L_d})$ and contracts as the speed of rotor increases.

When the operation is beyond base speed, the field weakening is employed so that the stator voltage will remains within the limit given by the equation (15). The d-axis and q-axis current is controlled such that it can satisfy the machine voltage limit given by

$$v_o = \sqrt{v_{do}^2 + v_{qo}^2} \leq V_{om} \quad (19)$$

Where, $v_{do} = -\omega_e L_q i_q$, $v_{qo} = \omega_e(L_d i_d + \Phi_{PM})$ and $V_{om} = V_{sm} - R_S I_{sm}$.

The relationship between i_d and i_q can be derived by the equation (17) by replacing V_{sm} by V_{om} in order to induce the effect of Stator Resistance drop. Therefore,

$$i_d = -\frac{\Phi_{PM}}{L_d} + \frac{1}{L_d}\sqrt{\frac{v_{om}^2}{\omega^2} - (L_q i_q)^2} \quad (20)$$

To control the current vector according to equation (20), the terminal voltage should be kept within V_{sm} in steady state. The intersection between the current limit and voltage limit trajectories at each speed provides the respective current limit for producing maximum torque at each operating speed. The operating point is located along the voltage limit curve. Therefore, the voltage limit curve decides the minimum current required to produce the desirable torque. The copper loss is also reduced in FW region. [2]-[3] These limit values are given by equation (21) and (22) respectively.

$$i_{dv} = -\frac{\Phi_{PM} L_d}{L_d^2 - L_q^2} + \frac{1}{L_d^2 - L_q^2}\sqrt{\Phi_{PM}^2 L_d^2 - (L_d^2 - L_q^2)(I_{sm}^2 L_q^2 + \Phi_{PM}^2 - \frac{V_{sm}^2}{\omega^2})} \quad (21)$$

$$i_{qv} = \sqrt{I_{sm}^2 - i_{dv}^2} \quad (22)$$

The trajectory of MTPA curve, the current limit curve, constant torque curves at different load and Voltage limit curve in FW region is shown in Figure (4).

4. Fuzzy Logic Controller rules for IPMSM:

The proposed FLC is implemented in MATLAB-Simulink using the Fuzzy Logic Toolbox. The inputs to the FLC are Speed error, Change in Speed Error and Actual Speed. The outputs of FLC are d-axis current (i_d) and q-axis current (i_q). The membership functions for inputs and outputs are shown in Figure (5)-(10). The inputs and outputs of FLC are scaled by appropriate gains such that the system perform efficiently.

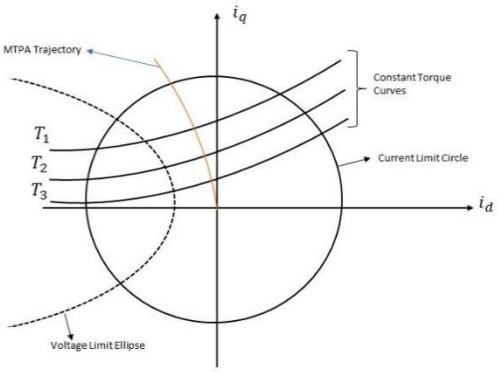

Figure 4 Limit Curves in FW operating Region

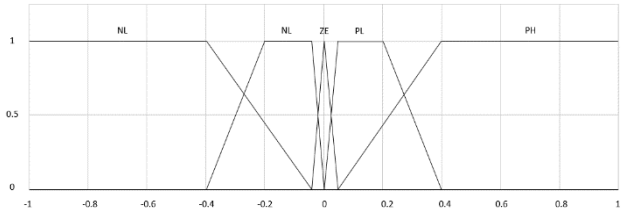

Figure 5 Speed Error Membership Function

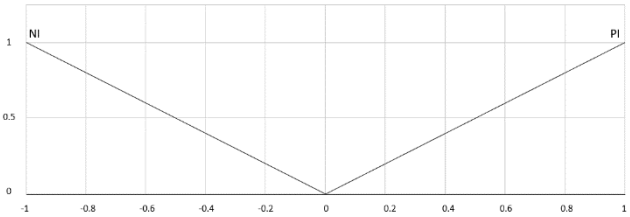

Figure 6 Change in Speed Error Membership Function

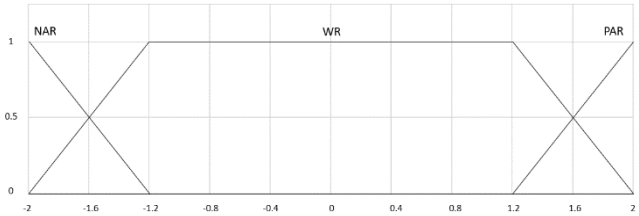

Figure 7 Actual Speed Membership Function

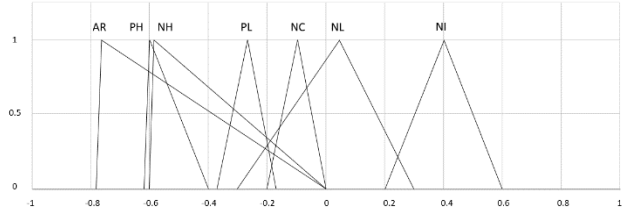

Figure 8 d-axis Current Membership Function

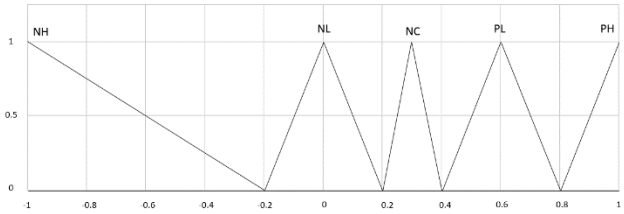

Figure 9 q-axis Current Membership Function

Rule 1: ***If*** *Δω is PH (positive high),* ***then*** i_q *is PH (positive high),* ***and*** i_d *is PH (positive high).*
Rule 2: ***If*** *Δω is PL (positive low),* ***then*** i_q *is PL (positive low),* ***and*** i_d *is PL (positive low).*
Rule 3: ***If*** *Δω is NH (negative high),* ***then*** i_q *is NH (negative high),* ***and*** i_d *is NH (negative high).*
Rule 4: ***If*** *Δω is NL (negative low),* ***then*** i_q *is NL (negative low),* ***and*** i_d *is NL (negative low).*
Rule 5: ***If*** *Δω is ZE (zero)* ***and*** ω_r *is WR (within range),* ***then*** i_q *is NC (not changed),* ***and*** i_d *is NC (not changed).*
Rule 6: ***If*** ω_r *is PAR (positive above rated)* ***or*** *NAR (negative above rated),* ***then*** i_q *is NL (negative low),* ***and*** i_d *is AR (above rated).*
Rule 7: ***If*** *Δω is ZE (zero)* ***and*** *Δe is PI (positive increase),* ***then*** i_q *is PL (positive low),* ***and*** i_d *is PL (positive low).*
Rule 8: ***If*** *Δω is ZE (zero)* ***and*** *Δe is NI (negative increase),* ***then*** i_q *is NL (negative low),* ***and*** i_d *is NL (negative low).*
Where,
Δω is change in rotor speed
ω_r *is rotor speed*
Δe is change in speed error

5. Results and Discussion

The whole drive system is simulated in MATLAB-Simulink under different load and Speed conditions. The whole drive system is shown in Figure (8). The simplified block diagram is shown in figure (11)[10]. The simulation parameters of IPMSM is given in table 1.

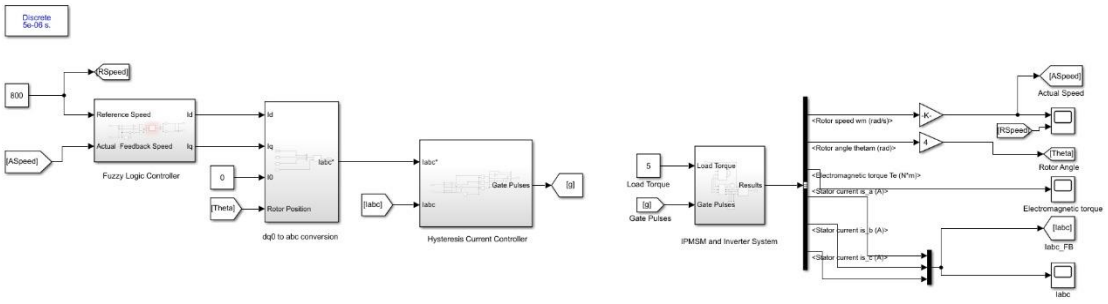

Figure 10 Drive System in MATLAB-Simulink

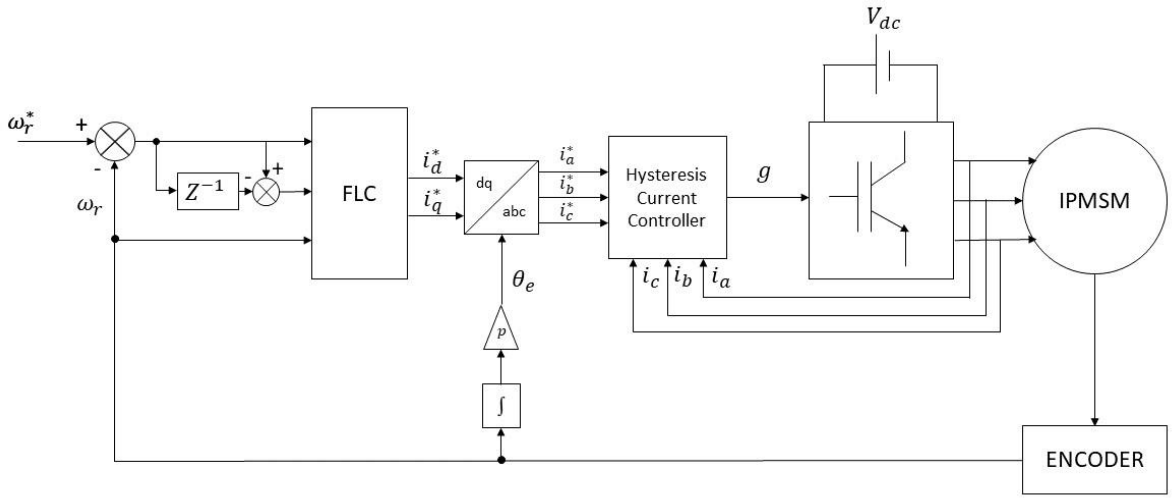

Figure 11 Simplified Block Diagram of Drive System

Table 1: IPMSM Simulation Parameters

Parameter	Parameter Value
Number of Pole Pairs	4
Stator Resistance	0.138 Ω
Permanent Magnet Flux Linkage	0.171 Vs
d-axis Inductance	0.00251 H
q-axis Inductance	0.00617H
Line Voltage (rms)	440 V
Phase Current (rms)	60 A
Base Speed	1500 rpm
Rated Torque	50 Nm
Friction Coefficient	0.00001
Rotor Inertia	0.04357 kg.m^2

The simulation is initiated by setting the constant 15 Nm load torque and step input of 1000 rpm reference speed. The desired speed 1000 rpm is reached without any overshoot or undershoot. The comparison of Reference Speed and Actual Speed is shown in Figure (12). The variation in reference speed is also made during the simulation. It changes from1000 rpm to 1500 rpm and then increased to 2000 rpm. The response are shown in figure (12).

The generated torque, d-axis and q-axis current waveforms and 3 phase current waveform if shown in figure (13), (14) and (15) respectively. The table 2 contains the important observations from the waveforms.

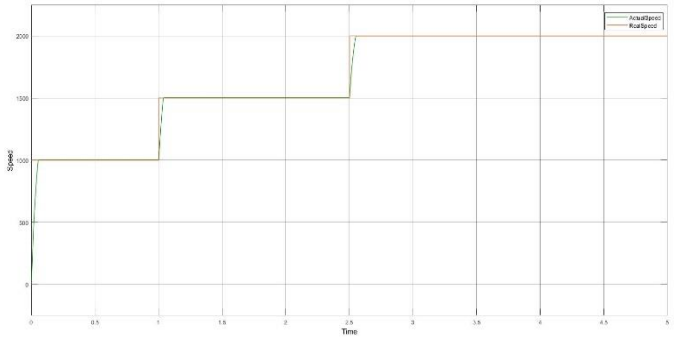

Figure 12 Speed Waveform

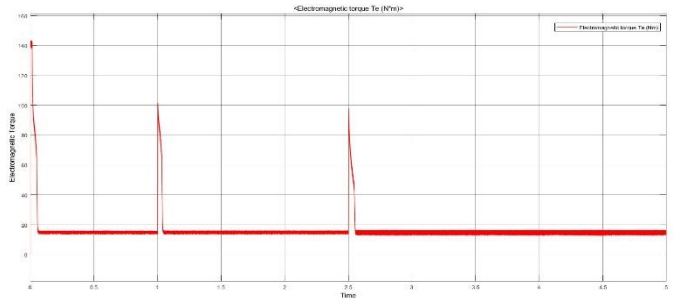

Figure 13 Generated Torque

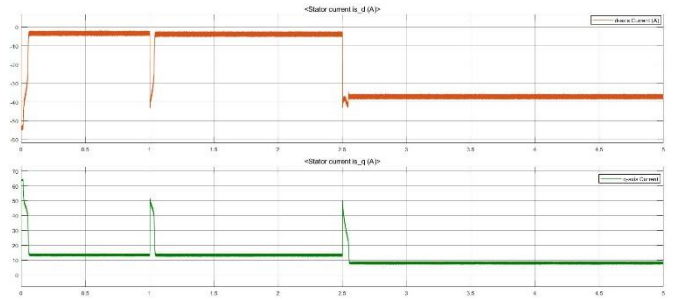

Figure 14 d axis and q axis Current

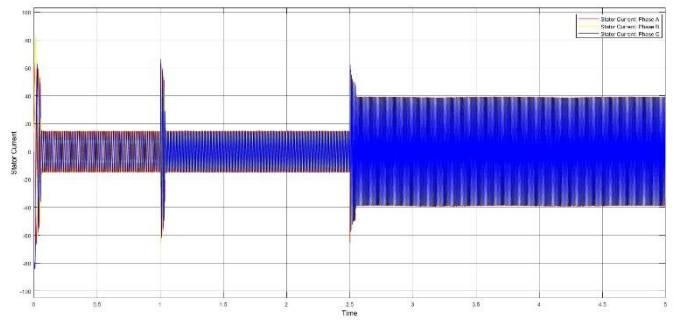

Figure 15 3-phase Current Waveform

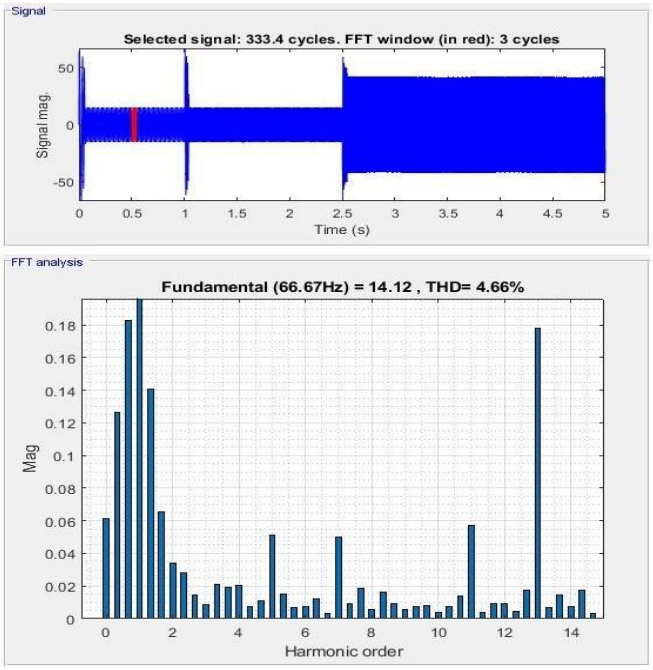

Figure 16 FFT Analysis at 1000 rpm

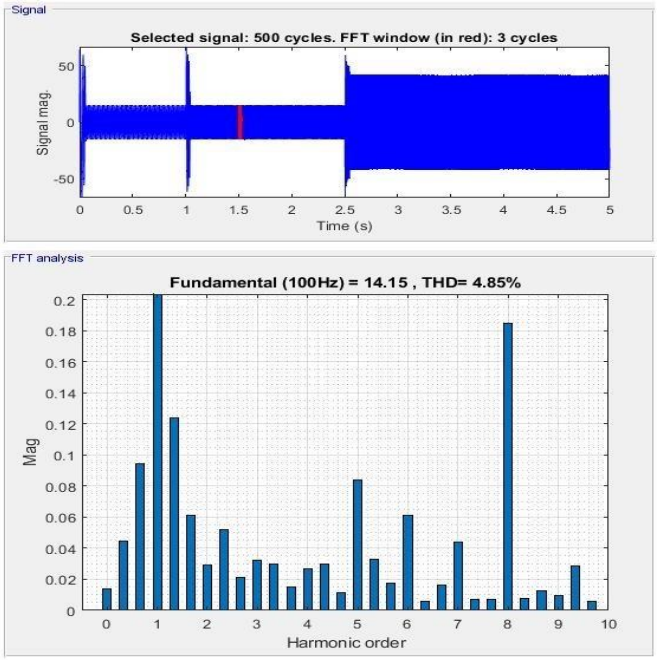

Figure 17 FFT Analysis at 1500 rpm

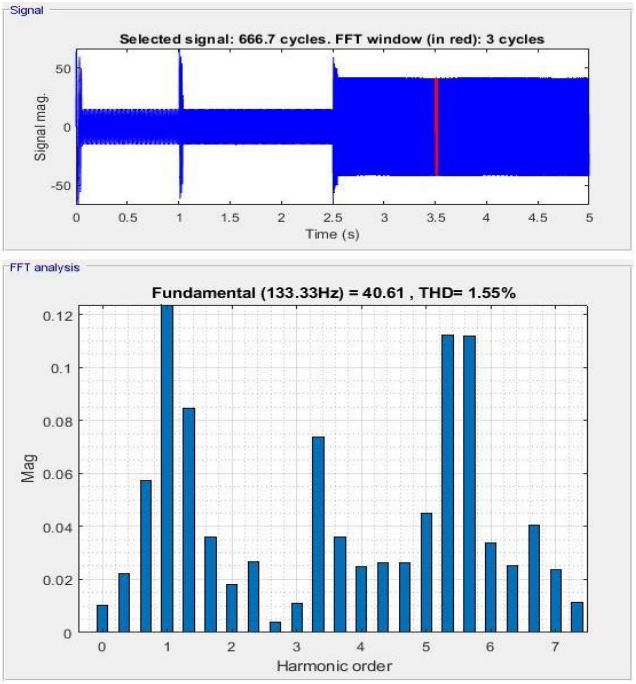

Figure 18 FFT Analysis at 2000 rpm

Other Transient Response Parameters like Rise time, Delay time, and Settling time are shown in Table (3). We can see from table (3) that the settling time, rise time and delay time is also reduced. So, we can get less transient effect during speed change. Total Harmonic Distortion (THD) in Line Current is shown in figure (16), (17) and (18) at different speed. The Steady State Response Parameters like Torque Ripple, THD, and Steady State Error (e_{ss}) in Steady State Condition is shown in Table (4). We can observe from Table (4) that during steady state condition ripple in torque, THD and steady state error in Speed are less.

Table 2: Simulation Table

Sr. No.	Time (s)	Speed (rpm)	I_d (A)	I_q (A)	Torque (Nm)	3-Phase Current (A)
1	0 to 0.057	0 to 1000	-54 (peak)	64 (peak)	143 (peak)	80 (peak)
2	0.057 to 1	1000	-3.72	14.04	15	9.55
3	1 to 1.04	1000 to 1500	-43.6 (peak)	51.8 (peak)	101 (peak)	60 (peak)
4	1.04 to 2.5	1500	-4.23	14.06	15	9.9
5	2.5 to 2.55	1500 to 2000	-43.57 (peak)	51.5 (peak)	97.5 (peak)	60 (peak)
6	2.55 to 5	2000	-37.5	8.5	15	26.87

Table 3: Transient Response Parameters

Sr. No.	Speed Change	0 to 1000 rpm	1000 to 1500 rpm	1500 to 2000 rpm
1	Rise Time	0.057 sec	0.04 sec	0.054 sec
2	Delay Time	0.021 sec	0.019 sec	0.023 sec
3	Settling Time	0.057 sec	0.041 sec	0.055 sec

Table 4: Steady State Response Parameters

Sr. No.	Speed	1000 rpm	1500 rpm	2000 rpm
1	Torque Ripple	6.67 %	6.67%	8.67%
2	THD	4.66%	4.85%	1.55%
3	Steady State Error (e_{ss}) in Speed	0.4%	0.25%	-0.04%

6. Conclusion

The entire drive system is simulated using MATLAB-Simulink and fuzzy logic toolbox. The proposed FLC can generate the reference current such that we can get the desire outputs in minimum time. We can also achieve minimum steady state error during running condition. The rise time and settling time of the system is minimum. The overshoots and undershoots in speed can be removed using the FLC.

Acknowledgements

We would thank Electrical engineering department of Birla Vishvakarma Mahavidyalaya for providing MATLAB licensed version software for simulation work. We would also thank Dr. Rukmi Dutta, Associate Professor, University of south wales, Sydney, Australia for providing motor data during training.

Appendix

A. We can improve the results by neural network method for controlling speed and torque.
B. We can use other controlled strategy other than hysteresis current loop method.
C. In Fuzzy rules, output can be change accordingly different membership functions.
D. Fuzzy algorithms can be implement on the hardware, so we can verify the simulation results with the hardware.

REFERENCES

[1] M. N. Uddin and M. M. I. Chy, "A Novel Fuzzy-Logic-Controller-Based Torque and Flux Controls of IPM Synchronous Motor," in IEEE Transactions on Industry Applications, vol. 46, no. 3, pp. 1220-1229, May-june 2010, doi: 10.1109/TIA.2010.2045334.

[2] Dehkordi, Behzad Mirzaeian and Kiyoumarsi, Arash and Hamedani, Pegah and Lucas, Caro, “A Comparative Study of Various Intelligent Based Controllers for Speed Control

of IPMSM Drives in the Field-Weakening Region," in Expert Syst. Appl., vol. 38, no. 10, pp. 12643–12653, September 2011, doi: 10.1016/j.eswa.2011.04.052.

[3] Rahman, F. and Dutta, R. (2013). Control of Interior Permanent Magnet Synchronous Machines. In AC Electric Motors Control, F. Giri (Ed.). https://doi.org/10.1002/9781118574263.ch19

[4] C. B. Butt, M. A. Hoque and M. A. Rahman, "Simplified fuzzy-logic-based MTPA speed control of IPMSM drive," in IEEE Transactions on Industry Applications, vol. 40, no. 6, pp. 1529-1535, Nov.-Dec. 2004, doi: 10.1109/TIA.2004.836312.

[5] M. J. Hossain, M. S. Hossain, M. A. Hoque and M. S. Anower, "A novel Fuzzy logic based flux weakening speed control for IPMSM drive with variable direct and quadrature axis inductances," 2007 10th international conference on computer and information technology, 2007, pp. 1-6, doi: 10.1109/ICCITECHN.2007.4579367.

[6] M. S. Hossain and M. J. Hossain, "Performance analysis of a novel fuzzy logic and MTPA based speed control for IPMSM drive with variable d- and q-axis inductances," 2009 12th International Conference on Computers and Information Technology, 2009, pp. 361-366, doi: 10.1109/ICCIT.2009.5407264.

[7] M. N. Uddin and M. A. Rahman, "High-Speed Control of IPMSM Drives Using Improved Fuzzy Logic Algorithms," in IEEE Transactions on Industrial Electronics, vol. 54, no. 1, pp. 190-199, Feb. 2007, doi: 10.1109/TIE.2006.888781.

[8] H. Wu, S. Wang and C. Gu, "Simplified fuzzy logic based flux weakening speed control of IPMSM drive," 2011 International Conference on Electrical Machines and Systems, 2011, pp. 1-4, doi: 10.1109/ICEMS.2011.6073883.

[9] R. Krishnan, "Permanent Magnet Synchronous and Brushless DC Motor Drives", Electrical and Computer Engineering Department, Virginia Tech Blacksburg, Virginia, U.S.A., CRC Press Taylor & Francis Group, 2010.

[10] Mohamed S. Zaky, "Robust Sliding Mode Speed Controller-based Model Reference Adaptive System (MRAS) and Load Torque Estimator for Interior Permanent Magnet Synchronous Motor (IPMSM) Drives", Electric Power Components and Systems, 2015, 43:13, 1523-1533, DOI: 10.1080/15325008.2015.1041624

[11] Mitsubishi Electrical inverter, "IPM TECHNICAL NOTE", Technical note no.3

[12] Rasmussen, P. O., and T. N. Matzen. "Torque Control in Field Weakening Mode." Institute of Energy Technology, Aalborg (2009).

[13] Kongchoo, Natthawut, Phonsit Santiprapan, and Nattha Jindapetch. "Mathematical Model of Permanent Magnet Synchronous Motor." Asia Pacific Conference on Robot IoT System Development and Platform 2020 (APRIS2020)

[14] Huang, Zhuoran, Cheng Lin, and Jilei Xing. "A Parameter-Independent Optimal Field-Weakening Control Strategy of IPMSM for Electric Vehicles Over Full Speed Range." IEEE Transactions on Power Electronics 36, no. 4 (2020): 4659-4671.

[15] Hou, Pengchao, Xingcheng Wang, and Yang Sheng. "Research on Flux-Weakening Control

System of Interior Permanent Magnet Synchronous Motor Based on Fuzzy Sliding Mode
Control." In 2019 Chinese Control And Decision Conference (CCDC), pp. 3151-3156. IEEE,
2019.
[16] Lan, Zhiyong, Fanxiang Shen, Gang Zhu, Cai Chen, Li Li, and Chuntang Cao. "A Novel
Control Method of Improved Flux-Weakening Trajectory for IPMSM." In 2019 22nd
International Conference on Electrical Machines and Systems (ICEMS), pp. 1-6. IEEE, 2019.
[17] Toosi, Saman, Mohammad Rezazadeh Mehrjou, Mahdi Karami, and Mohammad Reza Zare.
"Increase performance of IPMSM by combination of maximum torque per ampere and flux-
weakening methods." International Scholarly Research Notices 2013 (2013).
[18] Justo, Jackson John, Francis Mwasilu, Eun-Kyung Kim, Jinuk Kim, Han Ho Choi, and Jin-
Woo Jung. "Fuzzy model predictive direct torque control of IPMSMs for electric vehicle
applications." IEEE/ASME Transactions on Mechatronics 22, no. 4 (2017): 1542-1553.
[19] Dey, Tanmoy, Kaushik Mukherjee, and Prasid Syam. "Dynamic adjustments of the DQ axes
reference voltage limits during flux weakening and MTPA control of an IPMSM drive for an
EV application." In 2016 2nd International Conference on Control, Instrumentation, Energy
& Communication (CIEC), pp. 324-328. IEEE, 2016.
[20] Amornwongpeeti, Sarayut, Oleh Kiselychnyk, Jihong Wang, Ciprian Antaloae, Michail
Soumelidis, and Nirav Shah. "A combined MTPA and maximum efficiency control strategy
for IPMSM motor drive systems." In 2016 International Conference on Electrical Systems
for Aircraft, Railway, Ship Propulsion and Road Vehicles & International Transportation
Electrification Conference (ESARS-ITEC), pp. 1-6. IEEE, 2016.
[21] Rao, Dr EVC Sekhara. "Space vector modulated direct torque control of IPMSM
drive." International Advanced Research Journal in Science, Engineering and Technology 2,
no. 8 (2015).
[22] Gavilanes, Edwin Xavier Domínguez, and Carlos Enrique Imbaquingo Muñoz. "Vector

control for an interior permanent magnet synchronous machine with maximum torque per
ampere strategy." Revista Politécnica 35, no.1 (2015): 118-118.
[23] Meher, Hrushikesh, A. K. Panda, and Tejavathu Ramesh. "Performance enhancement of the
vector control based Permanent Magnet Synchronous Motor drive using hybrid PI-Fuzzy
logic controller." In 2013 Students Conference on Engineering and Systems (SCES), pp. 1-
6. IEEE, 2013.
[24] Mishra, Ambarisha, Jignesh Makwana, Pramod Agarwal, and S. P. Srivastava.
"Mathematical modeling and fuzzy based speed control of permanent magnet synchronous
motor drive." In 2012 7th IEEE Conference on Industrial Electronics and Applications
(ICIEA), pp. 2034-2038. IEEE, 2012.
[25] Hossain, Md Jahangir, M. Ashraful Hoque, and Kazi Khairul Islam. "Simplified fuzzy
control for flux- weakening speed control of IPMSM drive." Advances in Fuzzy
Systems 2011 (2011).[26] Hossain, Md Jahangir, M. Ashraful Hoque, and Kazi Khairul
Islam. "Simplified fuzzy control for flux-weakening speed control of IPMSM
drive." Advances in Fuzzy Systems 2011 (2011).
[27] Kang, Jun. "General purpose permanent magnet motor drive without speed and position
sensor." Yaskawa Electric Corp., Japan, Yaskawa Application Note WP. AFD (2009).